Modification of the damping rate of the oscillations of a dust particle levitating in a plasma due to the delayed charging effect

M. Y. Pustylnik,[1] N. Ohno,[2] S. Takamura,[1] and R. Smirnov[3]
[1]*Graduate School of Engineering, Nagoya University, Furo-cho, Chikusa-ku, 464-8603, Nagoya, Japan*
[2]*EcoTopia Research Institute, Furo-cho, Chikusa-ku, 464-8603, Nagoya, Japan*
[3]*MAE, University of California at San Diego, La Jolla, California 92093, USA*
(Received 5 July 2006; published 12 October 2006)

Dependence of the damping rate of the oscillations of the dust particles levitating in the sheath on the plasma parameters is investigated both theoretically and experimentally. Significant deviations of the damping rate from the values predicted by the Epstein formula are found in the experiment. The delayed charging effect is applied for the theoretical explanation of the experimental results. Qualitative agreement between the theoretical and experimental data is obtained.

DOI: 10.1103/PhysRevE.74.046402 PACS number(s): 52.27.Lw, 52.35.−g, 52.40.Kh, 52.75.Xx

I. INTRODUCTION

Complex (dusty) plasmas have recently attracted the attention of researchers as systems available for observation at the kinetic level and have been studied in many aspects, such as phase transitions, waves, response to different external influences, and instabilities [1–3]. One of the specific features of the complex plasma medium is that the electrostatic charge, accumulated on the surface of a dust particle is not constant, but is self-consistently connected to the conditions in ambient electron-ion plasma. In Ref. [4] it has been demonstrated that variability of the dust particle charge may lead to the nonpotentiality of the electrostatic force, supporting the dust particle against gravity and consequently may provide a mechanism by means of which the energy may be supplied to the dust subsystem. Dependence of the dust particle charge on the number density of the dust particles levitating in the plasma has been claimed as a possible reason of the dust-acoustic instability [5]. Similar effect has been taken into account in the theoretical treatment of dust acoustic modes in complex plasmas [6,7] and waves in electron-dust plasmas [8].

As the charge accumulated on dust particles depends on the surrounding plasma parameters, it will be changing if a dust particle moves in the nonuniform plasma medium. However, due to the finite charging time actual charge on the dust particle should be different from the equilibrium value. The faster the dust particle moves and the larger the gradients of the plasma parameters are the larger the difference is. This phenomenon is known as the "delayed charging effect" (DCE). The influence of DCE on different wave modes in strongly coupled complex (dusty) plasma has been treated in Refs. [9,10]. Recently large amplitude shock wave in a strongly coupled complex plasma has been considered theoretically with the inclusion of the DCE [11]. The DCE has been proposed to cause the self-excited oscillations of the dust particles [12] and the self-excited transverse dust lattice waves observed at low neutral gas pressures [13]. Theoretical treatment of the DCE in connection with the dust particles levitating in sheaths has been given in Refs. [14–16]. The DCE is still considered as the strongest candidate to explain the instability of dust particles levitating in plasma sheaths at low neutral gas pressure. Consequently we use the theoretical model based on the DCE for the comparison with our experimental findings.

The levitation of a dust particle in a sheath occurs mainly due to the balance of electrostatic force and gravity. If we consider small oscillations of a dust particle and take into account only the linear term of the electrostatic force, the motion of the dust will be governed by the harmonic oscillator equation

$$\ddot{z} + 2\beta\dot{z} + \omega^2(z - z_0) = 0, \tag{1}$$

where z is the current vertical position of the dust particle and z_0 is its equilibrium position, β is the damping factor, and ω is the eigenfrequency. Following Refs. [14,15], the eigenfrequency is expressed as follows:

$$\omega^2 = -\left.\frac{e}{m_d}\frac{\partial(EZ_d)}{\partial z}\right|_{z=z_0}, \tag{2}$$

where Z_d, m_d are the equilibrium dust particle charge and mass, respectively, and E is the local electric field strength. Usually it is accepted that the only phenomenon affecting the damping of the oscillations is the neutral drag. For a spherical dust particle the corresponding damping rate derived from the well-known Epstein formula [17] reads

$$\beta_{\mathrm{epst}} = \delta\frac{4}{\pi}\frac{p}{\rho v_{\mathrm{th}} a}, \tag{3}$$

where p is the neutral gas pressure, v_{th} is the thermal velocity of gas molecules, a and ρ are the dust particle radius and material density, respectively, and δ is the dimensionless factor, depending on the character of the scattering of the gas molecules on the surface of a dust particle. Obviously, β_{epst} does not depend on any of the plasma parameters and is always positive. However, DCE leads to the appearance of an additional term in the damping rate β_{DCE}, so that total damping rate is $\beta = \beta_{\mathrm{epst}} + \beta_{\mathrm{DCE}}$, where [14–16]

$$\beta_{\mathrm{DCE}} = \left. \frac{\tau_{\mathrm{ch}}}{2} \frac{eE}{m_d} \frac{\partial Z_d}{\partial z} \right|_{z=z_0}. \quad (4)$$

τ_{ch} here has the meaning of the charging time or the time required to compensate small deviations of the charge from its equilibrium value. Physical meaning of the influence of DCE on damping is the appearance of excess electrostatic force $eE\delta Z_d$ (δZ_d is the deviation of the actual dust particle charge from its equilibrium value), varying coherently with the dust particle velocity.

Unlike β_{epst}, DCE term of the damping rate is in strong dependence on plasma parameters and may be positive as well as negative, so that net damping rate may also acquire negative values. Negative β is supposed to be the reason for the instability, observed in Refs. [12,13]. As a measure of the instability the amplitude of the self-excited oscillations has been used in those works. The amplitude, however, depends not only on β, but also on the nonlinear terms of the electrostatic force, which are rather difficult to determine. Therefore, direct measurements of β, performed in this work, are supposed to give much more information about the physics of the instability. We should note that negative values of β are rather difficult to measure systematically. So, we performed measurements of positive β not so far from the instability threshold, where the dust particle exhibits stable levitation and, on the other hand, β is significantly different from β_{epst}. In Ref. [15] it has been shown, that β may be also quite sensitive to the details of the electron energy distribution function in the bulk, e.g., if the bulk plasma is bi-Maxwellian, equilibrium charge gradient $\partial Z_d/\partial z$, charging time τ_{ch}, and consequently β may be in strong dependence on the fraction of energetic electrons even if its value in the bulk plasma is several percent. This theoretical conclusion is also verified in this work.

II. EXPERIMENTAL SETUP AND PROCEDURE

We performed our experiments in a device named "Kagerou" [12–15]. Kagerou is a double plasma device with a vertically aligned stainless-steel cylindrical chamber 35 cm in diameter and 90 cm height (Fig. 1). The volume of the chamber is divided into two equal parts by a separation grid. In Kagerou the argon plasma is generated by a dc discharge with hot filaments and confined with a multicusp magnetic field at the periphery. For the present experiment the plasma is generated only in the target part. It has been shown that the electrons in the bulk plasma of Kagerou have a bi-Maxwellian distribution [18]. Electrons of two groups have significantly different temperatures. Those that have higher and lower temperature are called "hot" and "cold" electrons, respectively. There are three electrodes, that are used for the plasma generation: to the hot cathode we apply the voltage, accelerating primary electrons (U_c), anode voltage (U_a) determines the plasma potential and the separation grid (biased independently with the voltage U_{sg}) is sometimes used as an additional anode to control the fraction of energetic electrons [18]. Levitation of the dust particles is achieved over a metallic grid electrode, biased negatively with respect to the plasma and located on the axis of the chamber slightly above

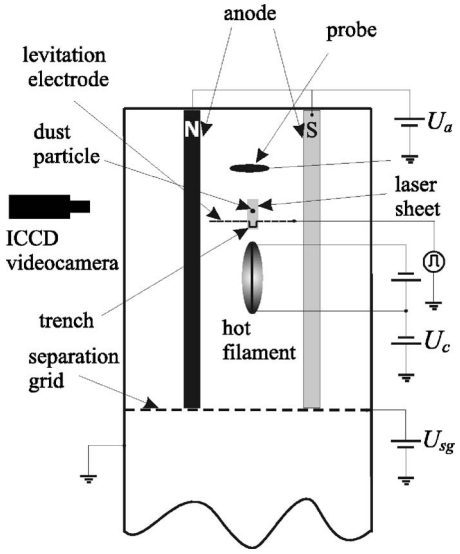

FIG. 1. Scheme of the experimental setup (side view). The anode plates (magnets) and the filaments are located at the periphery of the device and the levitation electrode and the probe are mounted on the axis. The function generator, connected to the levitation electrode provides the constant bias U_{le} for the levitation of the dust particles and an impulse to excite their oscillations.

the filaments. A long narrow trench in the electrode provides the confinement of the dust particles in the radial direction. The electrode is connected to the function generator, which supplies constant bias (U_{le}) as well as the impulse of voltage for the excitation of oscillations. The usual parameters of the impulse are amplitude 1 V and duration 10 ms.

Monodisperse polymethylmetacrylate ($\rho=1.22$ g/cm^3) dust balls 5 μm in diameter are supplied from a container, located above the electrode. Usually after one injection about 10–15 dust particles levitate. However, by applying several strong (4–5 V) impulses to the levitation electrode it is possible to achieve levitation of a single dust particle. Plasma parameters are measured with a plane disc-shaped Langmuir probe, located about 5 cm above the electrode. Details of the probe measurements are given in Ref. [18]. The range of experimental parameters in the present experiment is the following: discharge current $I=20-40$ mA, neutral pressure $p=0.1-0.8$ Pa, plasma density $n_0=(4-10)\times 10^8$ cm^{-3}, cold electron temperature $T_c\approx 0.3$ eV, hot electron temperature $T_h\approx 3$ eV, fraction of hot electrons $\alpha=(0.7-7)\times 10^{-2}$.

A levitating dust particle is illuminated with a He-Ne laser sheet and the scattered light is registered with an image-intensified CCD videocamera. Interference filter for the He-Ne laser wavelength is used to cut down the strong background light from the filaments. The frame rate of the videocamera is set to 250 fps and the exposure time to 2 ms. Spatial resolution of the imaging system is 13 μm/pixel. Start of the videorecord is synchronized with the application of the impulse to the levitation electrode. Digital movies of the dust behavior are recorded on hard disk of the computer. Position of a dust particle is determined in each frame and the obtained trajectory is analyzed.

If $|\beta| < \omega$, Eq. (1) has the solution

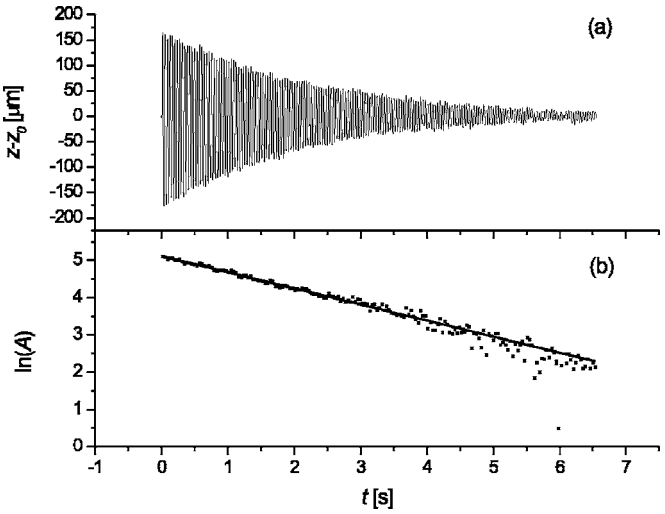

FIG. 2. (a) Example of a trajectory and (b) extracted amplitudes, fitted with a linear curve (solid line). Discharge current 40 mA, pressure 0.2 Pa, anode voltage 17 V, separation grid voltage 18 V. Damping factor $\beta=0.43\ \mathrm{s}^{-1}$.

$$z(t) = z_0 + A(t)\sin(\omega t + \epsilon), \tag{5}$$

where ϵ is the initial phase of the oscillations and $A(t)=A_0\exp(-\beta t)$ is the exponentially decreasing (in $\beta>0$ case we are dealing with) amplitude with the initial amplitude A_0. Therefore, to determine β from the experimental trajectory $z(t)$ [Fig. 2(a)] we first extract amplitude values $A(t)$ and fit the log-scale plot of A with a straight line [Fig. 2(b)].

III. THEORETICAL MODEL

Levitation of the dust particle and the delayed charging effect are determined by the structure of the sheath formed in front of the levitation electrode. Consequently, to evaluate β theoretically we need to formulate the sheath model. We use the standard collisionless approach with Boltzman distribution for both cold and hot electrons:

$$n_e = n_0\left[\alpha\exp\left(\frac{\phi_{\mathrm{pl}}-\phi}{T_h}\right) + (1-\alpha)\exp\left(\frac{\phi_{\mathrm{pl}}-\phi}{T_c}\right)\right], \tag{6}$$

where ϕ_{pl} is the plasma potential and ϕ is the local value of the sheath potential. For ions we employ the energy

$$\frac{m_i v_i^2}{2} + \phi = \frac{m_i C_s^2}{2} + \phi_0 = \phi_{\mathrm{pl}} \tag{7}$$

and the flux conservation

$$n_i v_i = n_{\mathrm{SE}} C_s, \tag{8}$$

where n_i, v_i, m_i are the ion density, velocity, and mass, respectively, ϕ_0, n_{SE} is the electrostatic potential and plasma density at the sheath entrance respectively, $n_{\mathrm{SE}}=n_e(\phi_0)$. C_S is the ion fluid velocity at the sheath entrance. It is connected with ϕ_0 via Eq. (7). Combining Eqs. (8) and (7), we obtain the following expression for the ion density:

$$n_i = n_{\mathrm{SE}}\sqrt{\frac{\phi_{\mathrm{pl}}-\phi_0}{\phi_{\mathrm{pl}}-\phi}}. \tag{9}$$

To determine the potential distribution we use the Poisson equation

$$\frac{d^2\phi}{dz^2} = 4\pi e(n_e - n_i). \tag{10}$$

We suppose that axis z points from the electrode into the bulk and $z=0$ at the electrode. Substituting the respective expressions for densities (6) and (9) and integrating once we obtain

$$\left(\frac{d\Phi}{dz}\right)^2 = 8\pi e\left(2n_{\mathrm{SE}}|\Phi_0|\left(\sqrt{\frac{\Phi}{\Phi_0}}-1\right) + n_0\left\{\alpha T_h\left[\exp\left(-\frac{\Phi}{T_h}\right)-\exp\left(-\frac{\Phi_0}{T_h}\right)\right] + (1-\alpha)T_c\left[\exp\left(-\frac{\Phi}{T_c}\right)-\exp\left(-\frac{\Phi_0}{T_c}\right)\right]\right\}\right), \tag{11}$$

where $\Phi=\phi_{\mathrm{pl}}-\phi, \Phi_0=\phi_{\mathrm{pl}}-\phi_0$. The generalized Bohm criterion [19] for our sheath reads

$$\frac{1}{m_i}\int_0^\infty n_{\mathrm{SE}}\frac{\delta(v-C_s)}{v^2} \le \left.\frac{\partial n_e}{\partial\Phi}\right|_{\Phi=\Phi_0}. \tag{12}$$

After some algebra it brings us to the following inequality:

$$n_0\left[\frac{\alpha}{T_h}\exp\left(\frac{\Phi_0}{T_c}\right) + \frac{1-\alpha}{T_c}\exp\left(\frac{\Phi_0}{T_c}\right)\right] + \frac{n_{\mathrm{SE}}}{2\Phi_0} \ge 0. \tag{13}$$

This allows us to determine Φ_0 and consequently C_s. In Ref. [20] the sheath in bi-Maxwellian plasma with the secondary emitting electrode has been considered; Eqs. (11) and (14) coincide with respective equations in Ref. [20] if the emission coefficients are set to zero.

Solving Eq. (11) with the boundary condition $\Phi(z=0)=\phi_{\mathrm{pl}}-U_{le}$ provides us the space potential distribution in the sheath. After calculating the potential profile we may calculate the profiles of electron and ion densities as well. This brings us to the calculation of the equilibrium charge, accumulated on a dust particle (Z_d). Z_d is the charge which provides the equality of electron and ion currents onto the surface of a dust particle. We use orbit-motion-limited (OML) [21] expressions for the electron current

$$I_e = -\pi a^2 n_0\left[\sqrt{\frac{8}{\pi}\frac{T_c}{m_e}}(1-\alpha)\exp\left(\frac{\Phi+\phi_f}{T_c}\right) + \sqrt{\frac{8}{\pi}\frac{T_h}{m_e}}\alpha\exp\left(\frac{\Phi+\phi_f}{T_h}\right)\right], \tag{14}$$

where m_e is the electron mass and ϕ_f is the equilibrium surface potential of a dust particle, and ion current

TABLE I. Example of the calculation of the parameters at the levitation point of a dust particle. Input parameters correspond to the probe-measured parameters at $I=40$ mA and $p=0.1$ Pa.

Input parameter	Value
U_{le} (V)	−6.0
U_{pl} (V)	1.3
n_0 (cm^{-3})	8.1×10^{8}
T_c (eV)	0.34
T_h (eV)	3.2
α	6.8×10^{-3}
Output parameter ($z=z_0$)	**Value**
z_0 (cm)	0.21
Φ (V)	−0.54
E (V/cm)	−8.5
ϕ_f (V)	−2.7
Z_d(e)	-4.7×10^{3}
τ_{ch} (s)	1.4×10^{-4}
β (s^{-1})	−0.13

$$I_i = \pi a^2 n_{\mathrm{SE}} C_s \left(1 + \frac{\phi_f}{\Phi}\right). \tag{15}$$

Ion temperature is assumed to equal the room temperature and consequently is neglected in comparison with the sheath space potential in the equation above. ϕ_f is determined from the condition $I_e+I_i=0$ and is connected with Z_d via the capacitance of a dust particle $Z_d=a\phi_f/e$.

Calculation of the profiles of equilibrium charge and electrostatic potential makes possible the calculation of the force distribution

$$F_{\mathrm{net}} = m_d g + EZ_d e \tag{16}$$

and finding the levitation point of a dust particle. To calculate β at the levitation point we have to determine the charging time. According to Ref. [22], the charging time may be determined as follows:

$$\tau_{\mathrm{ch}} = \frac{e\,\partial Z_d}{\partial(I_e + I_i)} = \frac{a}{\partial(I_e + I_i)/\partial\phi_f}. \tag{17}$$

We will assume $\delta=1.44$ in our calculations, according to Ref. [23], which gives a close value of δ for the neutral drag force on polymeric spheres in argon. This yields $\beta_{\mathrm{epst}}/p = 2.3$ s^{-1} Pa^{-1}. Typical results of the calculation are given in Table I.

IV. EXPERIMENTAL AND THEORETICAL RESULTS

A. Pressure variation

Let us now compare the experimental measurements and theoretical calculations of the damping rate. We performed two types of experiments. In the first one the separation grid was floating, $U_a=0$, $U_c=-80$ V, $U_{le}=-6$ V. We varied the neutral gas pressure and at every pressure we adjusted the filament heating current to keep the discharge current constant at every pressure. We performed this procedure at three values of the discharge current I 20, 30, and 40 mA. Results of probe measurements are shown in Fig. 3. At every pressure we could observe levitation we excited the oscillations of a levitating dust particle and measured the damping rate. On the other hand, using the probe-measured plasma parameters, we calculate the sheath structure and determine β theoretically according to the procedure described above. The results of the measurements and calculations are shown in Fig. 4. Instead of β we plot the ratio β/p. If Epstein drag is the only force responsible for the damping this ratio is not the function of neutral gas pressure according to Eq. (3). If forces of other nature become important for the damping, β/p should exhibit dependence on pressure.

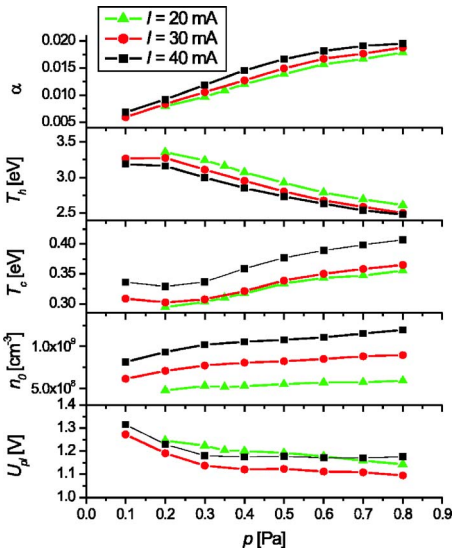

FIG. 3. (Color online) Variation of plasma parameters with pressure at floating separation grid, $U_a=0$, $U_c=-80$ V.

This dependence is clearly seen in Fig. 4. At pressures higher than 0.6 Pa both experimental and theoretical values

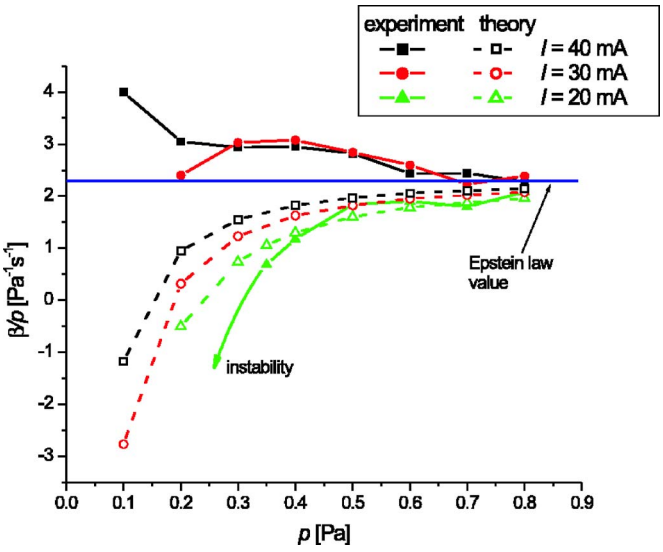

FIG. 4. (Color online) Dependence of ratio β/p on pressure. At lower pressures it significantly deviates from β_{epst}/p.

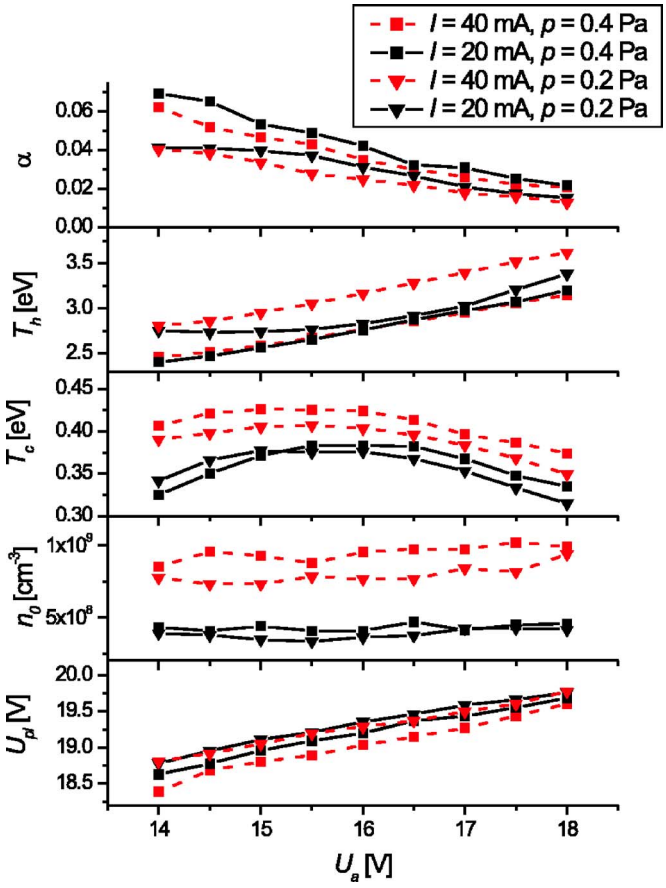

FIG. 5. (Color online) Variation of plasma parameters with anode voltage at $U_{SG}=18$ V, $U_c=-80$ V.

of β/p are quite close to the value, given by the Epstein formula (3). At lower pressures significant deviations from the Epstein value are observed. At $I=20$ mA, experimental value of β/p decreases with pressure and finally at $p=0.3$ Pa the dust particle becomes unstable. Therefore, we clearly observe decrease and change of sign of β. Experimental data at $I=20$ mA exhibits rather good agreement with theory. At $I=30$ mA β/p ratio first slightly increases with a decrease of pressure. However, at $p=0.2$ Pa β/p is close to the Epstein value and at $p=0.1$ Pa the dust particle becomes unstable and is dropped down. At $I=40$ mA experimental data shows the growth of β/p ratio up to the value of about $2\beta_{epst}/p$.Theory, however, predicts monotonic decrease of β/p ratio at all three values of current concerned.

B. Variation of α

In the second type of experiments we used the method of α variation, proposed in Ref. [18]. We kept $U_c=-80$ V, $U_{sg}=18$ V, and varied U_a in the range between 14 and 18 V. We performed this for $p=0.2$ Pa and $p=0.4$ Pa at discharge current 20 and 40 mA. Under these conditions variation of U_a from 14 to 18 V leads to an increase of α several times at slightly varying temperatures and almost constant plasma density (Fig. 5). At every value of U_a the damping rate of a dust particle could be measured and calculated theoretically. The respective data is plotted on Fig. 6. At $I=20$ mA and

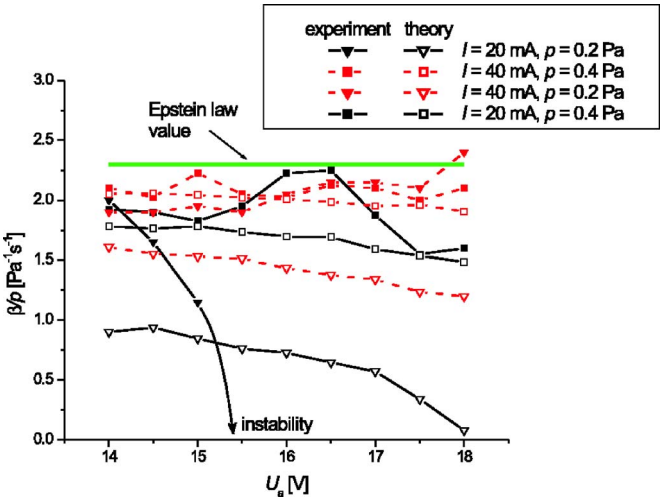

FIG. 6. (Color online) Dependence of ratio β/p on the anode voltage. At $I=20$ mA and $p=0.2$ Pa β/p strongly deviates from the value predicted by the Epstein formula.

$p=0.2$ Pa experimental data exhibits strong decrease of β/p with an increase of U_a (i.e., decrease of α). At $U_a=15.5$ V the dust particle becomes unstable. Therefore, we again observe the change of sign of β in the experiment. Theory, however, does not predict instability in this case. In other series β/p does not deviate from the Epstein value more than 30%.

Despite of sometimes significant disagreement with the DCE theory we should note that large deviations of the damping rate from the Epstein values are reported here. Also, the influence of the non-thermal energetic part of the EEDF on the behavior of dust particles levitating in plasma is evident from Figs. 5 and 6. This is another finding we would like to emphasize.

V. DISCUSSION

A. Comparison of experimental and theoretical results

Now we will try to discuss the obtained data in terms of DCE qualitatively. First of all it is obvious that deviation of the damping rate from Epstein value should be observed at low pressures. β_{epst} is proportional to p and consequently a decrease of p leads to a decrease of β_{epst} and β_{DCE} may become important.

A decrease of β with α observed on Fig. 6 may be explained by the influence of energetic electrons on the charging time of a dust particle. The dust particle usually levitates at a point that lies about 0.5 V below the plasma potential (see Table I). Also, the surface potential of a dust particle itself is about 3 V below the space potential at the levitation point. So, the surface potential is 3.5 V below the plasma potential. Consequently, only a few cold electrons from the bulk plasma may reach the surface of a dust particle. Energetic electrons play a crucial role in the charging of a dust particle. Reduction of their number unavoidably leads to an increase of τ_{ch} (Fig. 7) and consequently to a higher significance of DCE. Stronger deviation of β/p from the Epstein

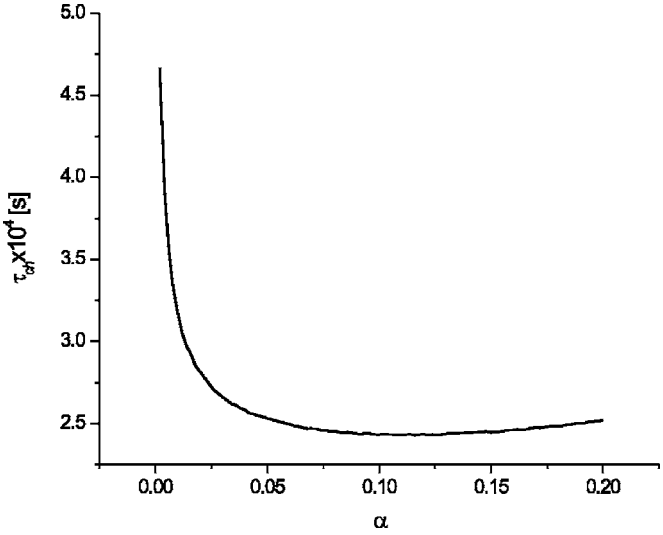

FIG. 7. Dependence of charging time on α. Calculation performed for $n_0=4\times10^8$ cm^{-3}, $T_c=0.3$ eV, $T_h=3$ eV, $\phi_{pl}-U_{le}=9$ V. Dramatic increase of τ_{ch} is supposed to be the reason of enhancement of the DCE at small values of α.

value in the pressure variation experiment compared to the U_a variation experiment may be also explained by lower α values and similarity of other parameters (compare the plasma parameters on Figs. 3 and 5).

We should note, that β_{DCE} may be negative as well as positive. The sign of β_{DCE} is governed by the product $R=E\frac{\partial Z_d}{\partial z}|_{z=z_0}$. Electric field is negative (i.e., directed towards the electrode) all through the sheath. $\frac{\partial Z_d}{\partial z}$ at the levitation position of a dust particle may change the sign [15]. At high values of α $\frac{\partial Z_d}{\partial z}|_{z=z_0}>0$, leading to $\beta_{DCE}<0$. As α is reduced $\frac{\partial Z_d}{\partial z}|_{z=z_0}$ becomes negative, leading to positive β_{DCE}.

In Fig. 8 a map of β_{DCE} in (n_0,α) plane at $T_c=0.3$ eV and $T_h=2.8$ eV is presented. We can clearly distinguish three regions on this map. First is the region where $\beta_{DCE}<0$. It occupies the major area of the map. Second is a narrow region of $\beta_{DCE}>0$. And the last is the region, in which levitation condition may not be satisfied. Neighborhood of $\beta_{DCE}>0$ and nonlevitatable regions is very natural. $\beta_{DCE}>0$ requires $\frac{\partial Z_d}{\partial z}|_{z=z_0}<0$. However, the stability of the levitation of a dust particle requires

$$\left.\frac{\partial(EZ_d)}{\partial z}\right|_{z=z_0} = Z_d\left.\frac{\partial E}{\partial z}\right|_{z=z_0} + R<0. \qquad (18)$$

The first term in Eq. (18) is always negative within the sheath. Consequently, if the charge gradient is negative and becomes too large in absolute value, R may become larger in absolute value than $Z_d\frac{\partial E}{\partial z}|_{z=z_0}$ and the stability of the levitation may be violated.

On the map (Fig. 8) we have plotted the points, at which β was measured in the pressure variation experiments. In the experiments we observed positive values of β_{DCE} at $I=30$ and 40 mA (Fig. 3). However, our experimental points are very far from region of positive β_{DCE}, predicted by theory. Approximately 4 times smaller value of α is required for our

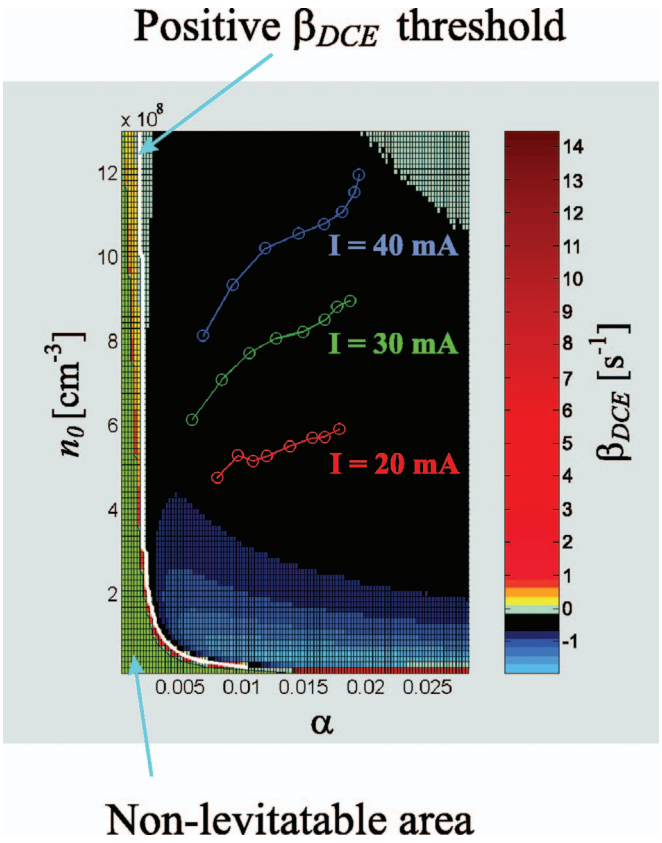

FIG. 8. (Color) Map of β_{DCE} in (n_0,α) plane. Color traces show the points, at which β was measured in a pressure variation experiment. White line represents the positive β_{DCE} threshold. In the green area levitation condition ($F_{net}=0$; $\partial F_{net}/\partial z<0$) cannot be satisfied within the sheath.

experimental points to enter this region. Also, we have checked that variations of T_c and T_h, which we observed in the experiments and which are not taken into account in the calculations of the map on Fig. 8, do not significantly affect the values of β_{DCE}. We should, however, note, that we observe $\beta_{DCE}>0$ at higher values of n_0. This is in accord with Fig. 8, since with the increase of n_0 the width of the α range, where $\beta_{DCE}>0$ increases.

B. Possible sources of discrepancy between the experiment and theory

1. Nonuniformity of the plasma

The major of the discrepancy in our opinion comes from the nonuniformity of the plasma in the vicinity of the levitation electrode. For our theoretical calculation of the sheath structure we used the plasma parameters measured by the probe about 5 cm above the electrode. We compared parameters at this point with the parameters measured approximately 5 cm below the probe [Fig. 9(a)]. Current-voltage characteristics with the subtracted ion current are given in Fig. 9(b). It is obvious that the electron saturation current is several times higher below the levitation electrode than above. This means that the plasma density increases in the downward direction. Also the currents of the energetic com-

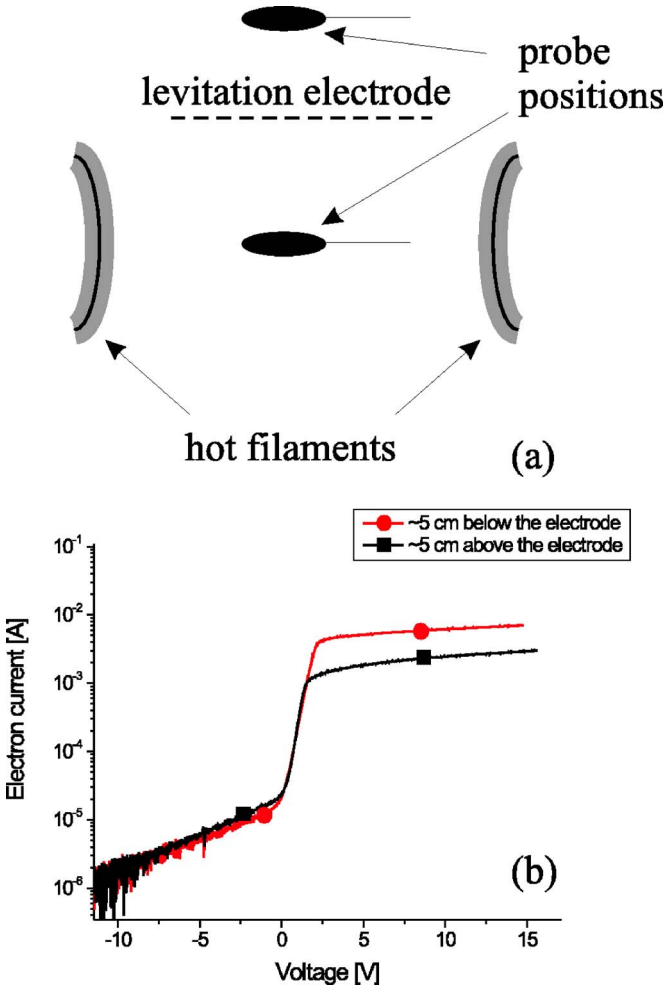

FIG. 9. (Color online) (a) Positions of the probe. Probe, located below the levitation electrode is in the plane with the filaments, so it indicates higher plasma density. (b) Comparison of the current-voltage characteristics at two positions. Below the levitation electrode the plasma density is several times higher compared to that above it; α exhibits opposite tendency.

ponent are almost same above and below the levitation electrode. This means, fraction of hot electrons α is higher above the electrode, than below, i.e., decreases in the downward direction. Consequently, the sheath, in which the dust particle levitates is governed by several times smaller α and several times higher n_0 compared to those we used for calculations. In terms of the color map on Fig. 8 this means that the experimental traces should be shifted in the upper-left direction and may approach the region of positive β_{DCE}.

2. Measurement and control accuracies

The error of probe measurements as well as the measurements of the damping rate has been found to arise mostly from the fitting procedures. Typical values are estimated as 25 and 20 % for the probe measurements and damping rate measurements, respectively. The accuracies of the control of discharge parameters are the following: current - 1 mA, pressure - 0.02 Pa, U_c - 0.5 V, other biasing voltages - 0.1 V.

3. Ion drag force

We have not taken into account the ion drag force. Our dust particles levitate in a sheath, where ions have to obey the Bohm criterion. Energy of the ion beam is supposed to be much higher, than the ion temperature, which is assumed to equal room temperature. Consequently, we may use cold ions approximation for the ion drag force in the sheath [22]. Also, it is important to note that our sheath is formed in the vicinity of a mesh electrode. Plasma exists on both sides of the electrodes and plasma particles may pass through the mesh. Consequently, total ion flux to the electrode is $(1-\kappa)n_{\mathrm{SE}}C_s$, where κ is the transparency of the electrode. Let us assume κ to equal the geometric transparency of the electrode. Then estimation gives us $\kappa=0.88$. If we calculate the ion drag force, using the data in Table I and the reduced ion flux, we will obtain $F_{\mathrm{dr}}\approx 0.04 m_d g$, which is negligible.

4. Shape of the ion velocity distribution function (VDF)

In our theory we used the cold ion approximation for the ion current to the dust particle (15). In reality, however, the ion VDF has a finite width, which in principle has to be taken into account in the calculation of an ion current to a dust particle.

To find out the importance of the finite width of the ion VDF we performed particle-in-cell (PIC) simulations of the sheath structure, using an originally developed one-dimensional code [24,25]. The simulated system of 2 cm length is bounded by the electrode on one side and by an interface with a bulk plasma on the other side. The bulk with given densities and VDF of electrons and ions provides input fluxes of plasma particles into the simulated system. We assume that sheath is symmetric on both sides of the levitation electrode. Consequently, the penetration of plasma particles through the mesh electrode can be effectively described as their reflection from the electrode back into the simulated system with probability given by κ. The bulk plasma boundary is fully transparent for outgoing plasma particles. A Monte Carlo extension of the PIC method [26] was used to simulate ion charge exchange and elastic collisions with neutral Ar atoms. The neutral gas at room temperature was supposed to be uniformly distributed in the system. The ion-neutral collision cross sections are given according to Ref. [27]. The simulations are performed sufficiently long time until the system becomes steady state. The code allows us to obtain local electron and ion VDFs at selected points.

We simulated the sheath structure for the data shown in Table I. The simulated ion VDF at $z=2$ mm (close to the levitation position according to Table I) is shown in Fig. 10(a). Electron and ion currents onto a dust particle are calculated as follows [21]:

$$I_{e,i} = \mp e\pi a^2 \int_{v_{e0},0}^{\infty} v_{e,i} f_{e,i}(v_{e,i}) \left(1 \pm \frac{2e\phi_f}{m_{e,i} v_{e,i}^2}\right) dv_{i,e}, \quad (19)$$

where $v_{e0}=\sqrt{2e\phi_f/m_e}$. The plot of the currents versus the surface potential at $z=2$ mm is shown in Fig. 10(b). The intersection point of electron and ion current curves gives the equilibrium potential of a dust particle. The figure clearly shows, that if the shape of the ion VDF is taken into account,

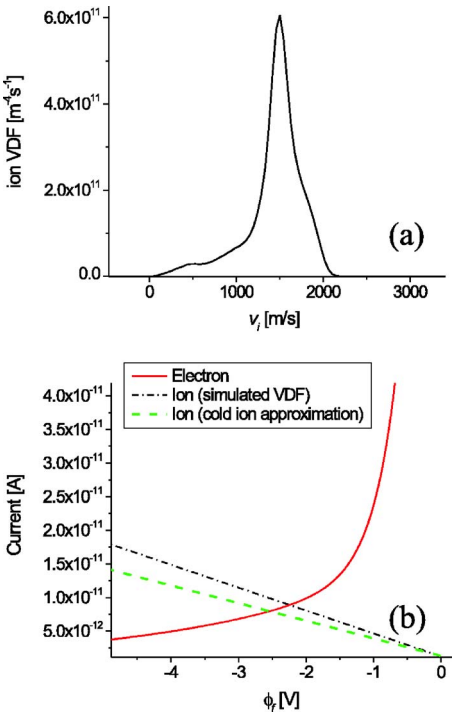

FIG. 10. (Color online) Simulated ion VDF (a) and currents onto a dust particle (b) at $z=2$ mm. Electron current and ion current, originating from the simulated ion VDF, are calculated with the help of Eq. (19). For the cold ion approximation case Eq. (15) is used with $\Phi=m_i v_{i\max}^2/2$, where $v_{i\max}$ is the ion velocity, for which f_i is maximum. The intersection point of electron and ion currents gives the equilibrium potential on a dust particle: −2.24 V for the simulated ion VDF case and −2.54 V for the cold ion approximation case.

the equilibrium potential on a dust particle is reduced about 12% with respect to the cold ion case.

VI. CONCLUSIONS

We have investigated the damping rate of the harmonic oscillations of a dust particle, levitating in an ion sheath, formed in the vicinity of an electrode immersed into the magnetically confined diffusion Ar plasma using the high-speed video recording of the dust particle motion. Theoretical consideration has been performed on the basis of the delayed charging effect. The structure of the sheath, confining a dust particle, has been calculated using the Bohm sheath theory with bi-Maxwellian electrons for the parameters of the bi-Maxwellian electron VDF in the bulk plasma, measured during the experiment. The damping rate of the harmonic oscillations has been calculated at the levitation position.

We have experimentally obtained the dependence of the damping rate on the neutral pressure. It has been found that at lower pressures the damping rate significantly deviates from the values predicted by the Epstein formula. The sign of the deviation depended on the bulk plasma density: at relatively smaller plasma density the measured damping rate was smaller than the predicted Epstein value; however, at relatively higher density the measured damping rate was higher than the predicted Epstein value. Our theory predicted the decrease of the damping rate at lower density as well as at the higher density at the experimentally measured plasma parameters. However, at the same time the theory predicted the existence of a narrow region of the increase of the damping rate at much lower fractions of energetic electrons. It has also been found that an increase of the fraction of energetic electrons leads to a decrease of the deviation of the damping rate from the Epstein value. Here we had qualitative agreement between theory and experiment.

Possible sources of the discrepancy between the experiment at theory are the following: nonuniformity of the plasma (fraction of energetic electrons and plasma density vary several times in the vicinity of the levitation electrode); accuracies of the measurements of plasma parameters and of the damping rate; taking into account the shape of the ion VDF, obtained by the PIC simulation of the sheath structure, was found to result in a reduction of the equilibrium surface potential of the dust particle of the order of 12%.

ACKNOWLEDGMENTS

One of the authors (M.Y.P.) acknowledges the financial support from the Japan Society for the Promotion of Science, Grant-in-Aid for Scientific Research 16-04072.

[1] V. E. Fortov, A. G. Khrapak, V. I. Molotkov, O. F. Petrov, and S. A. Khrapak, Phys. Usp. **47** (2004).
[2] V. I. Molotkov, O. F. Petrov, M. Yu. Pustyl'nik, V. E. Fortov, and A. G. Khrapak, High Temp. **42**, 827 (2004).
[3] V. E. Fortov, A. V. Ivlev, S. A. Khrapak, A. G. Khrapak, and G. E. Morfill, Phys. Rep. **421**, 1 (2005).
[4] V. V. Zhakhovskii, V. I. Molotkov, A. P. Nefedov, V. M. Torchinskii, A. G. Khrapak, and V. E. Fortov, JETP Lett. **66**, 419 (1997).
[5] V. E. Fortov, A. G. Khrapak, S. A. Khrapak, V. I. Molotkov, A. P. Nefedov, and V. M. Torchinsky, Phys. Plasmas **7**, 1374 (2000).
[6] A. V. Ivlev and G. E. Morfill, Phys. Plasmas **7**, 1094 (2000).
[7] X. Wang, A. Bhattacharjee, S. K. Gou, and J. Goree, Phys. Plasmas **8**, 5018 (2000).
[8] S. A. Khrapak and G. E. Morfill, Phys. Plasmas **8**, 2629 (2001).
[9] A. Mishra, P. K. Kaw, and A. Sen, Phys. Plasmas **7**, 3188 (2000).
[10] P. K. Kaw, Phys. Plasmas **8**, 1890 (2001).
[11] S. Ghosh, Phys. Plasmas **13**, 022301 (2006).
[12] S. Nunomura, T. Misawa, N. Ohno, and S. Takamura, Phys. Rev. Lett. **83**, 1970 (1999).
[13] T. Misawa, N. Ohno, K. Asano, M. Sawai, S. Takamura, and P.

K. Kaw, Phys. Rev. Lett. **86**, 1219 (2001).
[14] T. Misawa, S. Nunomura, N. Ohno, and S. Takamura, J. Appl. Phys. **39**, L551 (2000).
[15] S. Takamura, T. Misawa, N. Ohno, S. Nunomura, M. Sawai, K. Asano, and P. K. Kaw, Phys. Plasmas **8**, 1886 (2001).
[16] A. V. Ivlev, U. Konopka, and G. Morfill, Phys. Rev. E **62**, 2739 (2000).
[17] P. S. Epstein, Phys. Rev. **23**, 710 (1924).
[18] M. Pustylnik, N. Ohno, and S. Takamura, Jpn. J. Appl. Phys., Part 2 **45**, 926 (2006).
[19] M. A. Lieberman, and A. J. Lichtenberg, *Principles of Plasma Discharges and Materials Processing* (Wiley, New York, 1994).
[20] T. Gyergyek and M. Cercek, Contrib. Plasma Phys. **45**, 89 (2005).
[21] H. M. Mott-Smith, and I. Langmuir, Phys. Rev. **28**, 727 (1926).
[22] T. Nitter, Plasma Sources Sci. Technol. **5**, 93 (1996).
[23] B. Liu, J. Goree, and V. Nosenko, Phys. Plasmas **10**, 9 (2003).
[24] R. Smirnov, Y. Tomita, T. Takizuka, A. Takayama, and Yu. Chutov, JPFR Ser. 6, 752 (2003).
[25] R. Smirnov, Y. Tomita, T. Takizuka, A. Takayama, and Yu. Chutov, Contrib. Plasma Phys. **44**, 150 (2004).
[26] C. K. Birdsall, IEEE Trans. Plasma Sci. **19**, 65 (1991).
[27] Atomic and Plasma-Material Interaction Data for Fusion edited by R. K. Janev (IAEA, Vienna, 1998), Vols. 7A, 7B.